# Optimization of Reactive Power Dispatch Considering DG Units Uncertainty by Dandelion Optimizer

Mohammed Hamouda Ali‡*, Ahmed Mohammed Attiya Soliman*
Mohammed Fathy Ahmed*, Ahmed Hassan Adel*

[*] Electrical Engineering Department, Al-Azhar University, Cairo,Egypt

(Eng_MohammedHamouda@azhar.edu.eg,eng_ahmed1020@azhar.edu.eg,

mohamed.ahmed89@azhar.edu.eg, ahmed.adel@azhar.edu.eg)

‡ Corresponding Author; Mohammed Hamouda Ali, P.O. Box 11651, El Nasr St, Nasr City, Cairo, Egypt, Eng_MohammedHamouda@azhar.edu.eg

*Received: 26.10.2022 Accepted:27.11.2022*

**Abstract-** The optimal reactive power dispatch (ORPD) is a vital problem widely discussed in power system engineering, where ORPD is located as one of the optimal power flow (OPF) sub-difficulties which is a complex and nonlinear problem. The main motivation of this work is to study the secure and reliable functioning of electrical systems which has grown hard due to increased strained operating circumstances. As a result, there are more real and reactive power losses in the transmission network and a voltage fluctuation problem at the load bus because the development of generating and transmission systems has not kept pace with the increase in load. For optimal operation, the voltage at the load bus should be constant. Voltage fluctuation is linked to the power system's reactive power constraints. As a result, controlling the system's reactive power is critical. Additionally, the modern power system networks should be including renewable energy sources (RESs) to achieve benefits for both the utilities and the customers, i.e., technical, economic, and environmental including saving world fuel, saving transmission, and distribution costs, and reducing wholesale electricity prices. However, it rise network reservations due to haphazard behavior, accordingly that optimal power flow is not elongated approachable, and the probabilistic optimal reactive power dispatch (PORPD) necessity remains studied. This paper explains solving for a PORPD problem using the Taguchi orthogonal array technique (TOAT) or Taguchi method (TM) based on orthogonal arrays (OAs) for modeling and correlation between uncertainties of the RESs and using a new optimization algorithm to increase processing speed and accuracy. A new metaheuristic algorithm named the Dandelion optimizer (DO) has been proposed for the first time to solve the ORPD problem on the standard IEEE 30 bus and defined the optimal combination of dispatchable and non-dispatchable sources to make the most of several techno-economic and societal paybacks at the same time. Reactive power losses in power systems can be reduced by optimizing reactive power outputs from sources, transformer tap settings, and other compensating devices. The optimization of real and reactive powers and the installation of RES at appropriate buses can minimize the losses and improve the voltage profile. Power loss minimization, voltage regulation, improvement in system reliability and readability, improved power quality, relieving transmission and distribution networks, and increased overall energy efficiency are among the major technical benefits of ORPD in presence of RES. The simulation outcomes employing the new proposed algorithm through the IEEE 30-bus test system and compared its performance with the results from other algorithms such as the Genetic algorithm (GA), Killer Whale Algorithm (KWA), Prairie dog optimization algorithm (PDO) and Whale optimization algorithm (WOA), prove that the DO optimizer is the most superior among all and lead to minimizing voltage deviation and power losses through high speed and minimum calculation time. Finally, the results prove that the proposed algorithm can be applied to a wide range of real-world optimization problems successfully.

**Keywords** Optimal Reactive Power Dispatch (ORPD), Distributed Generation (DG), Probabilistic Optimal Power Flow (POPF), Taguchi Method (TM), Orthogonal Arrays (OA), Dandelion Optimizer (DO).

## 1. Introduction

The electric power system is humanity's largest structure, divided into three major sections: generation, transmission, and distribution [1]. The generation section is a power plant that uses generators to generate both active powers in addition reactive. The active power is determined through the speed of the turbines in addition amount of fossil fuel used, whereas the reactive power is determined by the exciter circuit current of the synchronous generator [2]. Reactive power is critical in any section of the power system because if it is not present, the power system's operation and stability will suffer [3]. In distribution systems, any load type, such as R or R-L, R-C, or another type that has an inductor and works with magnetic fields, such as inductive machines, requires reactive power to spin [4]. When loads use reactive power, the power factor (PF) changes, which influences network losses, so power factor correction (PFC) is necessary to improve PF to close a unity value that represents the perfect and ideal state, where in this condition reactive power not used, and network losses are reduced and this compensation or reactive power injection based on capacitors [5],[6]. With a large power system containing many loads, transformers, generators, and other equipment, it remains critical to control the reactive power, therefore using the optimal power flow (OPF) to control reactive power is required. OPF mentions scheming in a cost-effective also stable operation, which is reached by correctly tuning the system's control variables and introducing elucidation that accomplishes the smallest objective function such as minimization of reactive power while taking system constraints [7]. Where OPF is acritical and nonlinear complex optimization problematic for evaluating the dependability and security of power schemes, several optimization techniques developed to solve the OPF topics. Avoiding obstacles and drawbacks for conventional methods, metaheuristic methods are used such as genetic algorithm [8], ant colony algorithm [9], particle swarm optimization PSO algorithm [10], ICA algorithm [11], in addition, monkey algorithm [12].

As the world population grows, the availability of fossil fuels decreases, posing a problem for power plants that generate electricity. These power plants pollute the air and cause other environmental issues [13]. In recent decades, the use of distributed generation (DGs) in electricity generation has grown [14]. Because DGs inputs are such as sunlight in photovoltaic (PV) cells and wind turbines (WT), DGs can settle down anywhere in the network that needs power, and their random and probabilistic nature increases the power system or distribution network uncertainty [15]. So, with the proliferation of DGs in power systems and even distribution networks, they change grids into smart grids that need OPF, which is a very important tool, so first uncertainty must be converted to a specific value and in smart grids, we cannot use the OPF, so we use probabilistic OPF [16, 17]. Due to the circumstances of DGs, the use of a meta-heuristic optimization scheme is better compared to other traditional methods because of their advantages including high speed and accurate calculation and many iterations don't trap in local optimum answer finally reaches the global solutions [18]. However, it is difficult to calculate many iterations and many mathematical processes using classic optimization algorithms or techniques such as Lagrange [19, 20] or Kuhn-Tucker conditions [21, 22], second-order cone relaxation [23], General reduced gradient method [24] and others, that we may eventually be trapped in local optimum solutions [25]. Probabilistic assessment methods are used for converting the DGs uncertainties such as Latin hypercube [26], point estimate method [27], scenario-based method [28], and Monte Carlo simulation (MCS) method which represents the basic technique for any probabilistic assessment method [29].

The literature review is reviewed below and present the application of different methods and optimization techniques in different ORPD problem with and without these DGs uncertainties conditions. Where in [30], combining the PSO algorithm with the genetic algorithm (GA) and Genetic PSO algorithmis formed, and the Hybridization of the Genetic PSO Algorithm with the Symbiotic Organisms Search (SOS) Algorithm has been finished to get the proposed (HGPSOS) algorithm used to solve the RPD problematic and applied in IEEE 30, bus testing scheme, wherever smallest power loss, smallest voltage aberration, and improvement voltage stability has reached.T. T. Nguyen *et al.* in [31] solving ORPDproblem with upgraded societal spider optimization (ISSO) algorithm and realizing dissimilar objectives, the improvement in the proposed method is confirmed by solving benchmark optimization functions, IEEE 30-bus system and IEEE 118-bus system and considering three independent objectives including power loss and voltage deviation minimization, and voltage stabilization enhancement.

In [32] authors implement the water wave optimization (WWO) algorithm on IEEE 30-bus to confirm the viability and feasibility of the WWO algorithm to treat the ORPD problem and results shows that it has better general behavior to decrease the real power losses. Zelan Li *et al.* [33] authors using an innovative improved antlion optimization algorithm (IALO) for resolving the ORPD problem and optimizing three single objective functions of three different IEEE with 30, 57, and 118 buses including total power loss and voltage deviation minimization and the index of Voltage stability (L-index) enhancement through significantly best optimal solutions. Lian In [34] proposed an adaptive multi-objective optimization artificial immune algorithm (AMOAIA)for reactive power optimization and tested it on an IEEE-30 bus, results prove that it can sensibly allocate reactive power based on ensuring the stability boundary of a convinced maximum static voltage stability index, while the power losses could be a reduction, in which could have improved voltage level.

In [35] the Rao-3 optimization algorithm is used to explain the inhibited non-linear ORPD problem given uncertainties owing to the variation continuously and the normal termination of wind speed and solar irradiation employing load demand variation. The proposed algorithms are authenticated via three standard IEEE trials with 30, 57, and 118-buses, the results providing the success of the proposed single-multi objective algorithms in explaining the deterministic and stochastic ORPD.

In [36] the heat transfer optimization (HTO) algorithm and simulated coronary circulation system (SCCS) optimization algorithm has been projected to explain the ORPD, anywhere with and without L-index (voltage stability), HTO and SCCS algorithm's cogency are proved in IEEE 30 bus and get Power loss minimalized, voltage deviation also decreased, and voltage stability index improved. Hamza Yapici author in [37] proposed an improved version of the pathfinder algorithm (PFA) for solving the ORPD and minimizing the power losses. Mathematical analyses are done on (57-118) bus IEEE standard testing power systems. To illustrate, the enhancement of the modified pathfinder algorithm (mPFA), roughly known methods are applied for comparison. Statistical tests are done to assess the consistency and status of the planned technique. Authors in [38] proposed an optimization algorithm named chaotic turbulentflow of water-based optimization (CTFWO) algorithm as a tool to solve the (ORPD) by minimizing the voltage and total power loss in dual IEEE, a (30- 57) bus systems. The Probabilistic Load Flow (PLF) problem with uncertainties considering the network load changes is solved using the optimal nonlinear complementary problem method [39].

Two- Point Estimation Method (2PEM) is used to solve Monte Carlo simulation (MCS) problems, which has a low computational load and requires only the initial statistical torques of the Random Variables (RVs) to analyze the problems, and the improved (2PEM) is used as a new evaluation method for modeling uncertainties by considering correlation as presented in [40]. To consider the correlation between WT and PV in the distribution network Taguchi Method (TM) is introduced in [41], where the PLF problem has been studied using (TM) for the IEEE standard 34-bus test system in which the three-phase voltages are unbalanced by considering the correlation between the input (RVs) and the results by 3PEM and 2PEM and MCS are compared and it is concluded that the response of the Taguchi Method (TM) for two levels and three levels of (RVs) are equal to the results of 2PEM and 3PEM, respectively, and that objective function is to reduce the overall cost.

In [42], in the IEEE 30-bus test network, based on Orthogonal Arrays (OAs)-using TM the POPF is analyzed by considering the correlation of uncertainties caused by input RVs. Where TM calculates and adjusts the optimal values of the input RVs, then the control variables of the POPF problem are adjusted to optimal values based on the optimal values of RVs using optimization GA to achieve the objective function and reduce system power losses, where Optimization ensures that the amount of losses is not stuck in the local optimal domain and is located in the global optimal domain and the global optimal is absolute and also the optimal output response is more reliable, because the losses are the least amount.

In [43], a novel two-stage optimization outline including A modified (TM), in mixture with a node precedence list, is proposed to calculate the optimal-mix integration of dispatchable (DG), and the planned approach is applied to two standard distribution schemes of 33 and 118 buses and results meaningfully advance the robustness and worldwide searching capability of TM.

In [44], based on the IEEE 13 nodes system a relative analysis is completed among three statistical techniques (Taguchi's Orthogonal Array Testing method (TOAT), Monte Carlo, and Two-Point method) by mixing the uncertainty of primary sources generation of renewable in power systems, and results from the previous survey suggestively advance the robustness and worldwide searching capability of Taguchi Method (TM).

To summarize, the main contributions of this research are:

- Taguchi method based on orthogonal arrays has been used for modeling the uncertainty of RESs and loads.
- A new metaheuristic algorithm named Dandelion optimizer (DO) algorithm has been proposed for the first time to solve a real-world optimization problem such as the ORPD problem.
- In DA, dandelion populations are designed with a Levy mutation, which can help to avoid falling into the local minima.
- This research assesses the work in two directions in addition to optimal RESs allocation. The first part examines the influence of the uncertainty of RESs and loads by using TM, while the second part discusses the optimal siting of all control variables for handling the ORPD problem.
- The efficacy of the outcomes of this approach has also been demonstrated in terms of lowering real and reactive power losses and meliorative voltage deviation considering distinct restrictions.
- The performance of the methodology proposed has been Verified using the typical test system IEEE 30 bus to detect its superiority for handling the problems and compared to other published approaches.
- The search efficiency, accuracy, and convergence speed of DO are validated and compared against well-established GA, KWA, PDO, and WOA algorithms. The proposed DA has a much faster speed than the GA, the KWA, the PDO, and the WOA.

This paper's organization is as presented: sector 2 presents the problem formulation of the ORPD. Sector 3 presents the uncertainty modeling for load demand, wind speed, and solar Irradiation. The (TOAT) method, and (DO) proposed algorithm are discussed in sectors 4,5 respectively. Also, sector 6 covers the simulation results. In this sector, analysis and comparison are done in contradiction of the nominated metaheuristic algorithms. Sector 7 presents the final discussion and conclusion.

## 2. Problem Formulation

The objective function of OPRD is to minimize network active power losses ($F_1$), minimize network reactive power losses ($F_2$).and minimize network voltage deviations ($F_3$) The problem is also formulated as an optimization problem in which the objective functions are expressed as (1), (2),and (3):

$$F_1 = min\, P_L = \sum_{i=1}^{nl} G_{ij}\left(V^2{}_i + V^2{}_j - 2\, V_i V_j \cos\theta_{ij}\right) \quad (1)$$

$$F_2 = min\, Q_L = \sum_{l=1}^{nl} Q_{Loss,l} = imag\ STL \quad (2)$$

$$F_3 = min\, VD = \sum_{i=1}^{NPQ} |V_i - 1| \quad (3)$$

Where $STL$ is the network apparent power, $Q_{Loss,l}$ is the total branch reactive power and $nl$ is the total number of network branches or transmission lines, and the load bus number is $NPQ$. The minimization of these objective functions is bound by various constraints [31-34]. Equations (4) and (5) show equal limits in the network, in these constraints $P_{Gi}$ and $Q_{Gi}$ are the amount of active and reactive power produced in the slack bus, respectively. $P_{Di}$ and $Q_{Di}$ are also the active and reactive demands of the buses. The denominator $V_i$ indicates the voltage of the bus i as well as the $\theta_{ij}$ $is$ amount of angle difference between the buses $i$ and the j. And $nb$-1 indicates all buses except slack bus. $Gij$ and $Bij$ are also the mutual conduction and suspension between buses i, j. Equations (6), (7), and (8) express unequal constraints including the active power ($P_{Gi}$), reactive power ($Q_{Gi}$), and voltage constraints of generators ($V_{Gi}$), in these unequal constraints NG represents the number of generators, $where\ P_{Gi}{}^{min}$ and $P_{Gi}{}^{max}$are the minimum and maximum active output power of bus i, $Q_{Gi}{}^{min}$ and $Q_{Gi}{}^{max}$are the minimum and maximum reactive output power of bus i, $V_{Gi}{}^{min}$ and $V_{Gi}{}^{max}$ are the minimum and maximum voltage allowed range at bus *i*. The taps of the transformers are also limited in their minimum and maximum range as follows (9). Where *NT* is the number of transformers, $T_i{}^{min}$ and $T_i{}^{max}$ are taps ratio of transformers settings with the minimum and maximum bounds. The constraints of shunt capacitor bank compensators are also as follows in equation (10). In this regard, *NC* is the number of compensators, $Q_{Ci}$ of reactive power generated, $Q_{Ci}{}^{min}$ and $Q_{Ci}{}^{max}$ are the minimum and maximum allowable reactive power compensation. In addition to these restrictions, according to equation (11), the constraints of load voltage ($V_{Li}$) must be kept within tolerable limits with minimum and maximum values $V_{Li}{}^{min}, and\ V_{Li}{}^{max}[45-46]$.

$$P_{Gi} = P_{Di} + |V_i| \sum_{j=1}^{nb} |V_j| (G_{ij} \cos\theta_{ij} + B_{ij} sin\theta_{ij}) \quad (4)$$

$$Q_{Gi} = Q_{Di} + |V_i| \sum_{j=1}^{nb} |V_j| (G_{ij} \sin\theta_{ij} - B_{ij} cos\theta_{ij}) \quad (5)$$

$$P_{Gi}{}^{min} \le P_{Gi} \le P_{Gi}{}^{max} \quad , i=1,2,..,NG \quad (6)$$

$$Q_{Gi}{}^{min} \le Q_{Gi} \le Q_{Gi}{}^{max} \quad , i=1,2,..,NG \quad (7)$$

$$V_{Gi}{}^{min} \le V_{Gi} \le V_{Gi}{}^{max} \quad , i=1,2,..,NG \quad (8)$$

$$T_i^{min} \le T_i \le T_i^{max} \quad , i=1,2,..,NT \quad (9)$$

$$Q_{Ci}{}^{min} \le Q_{Ci} \le Q_{Ci}{}^{max} \quad , i=1,2,..,NC \quad (10)$$

$$V_{Li}{}^{min} \le V_{Li} \le V_{Li}{}^{max} \quad , i = 1,2,..,NPQ \quad (11)$$

## 3. Uncertainty modelling

In probabilistic planning, it is important to state an appropriate statistical model for RVs. Therefore, the Continuous Probability Function (PDF) is for modeling the uncertainty of the system, which contains doubt in the demand of load, the production of solar PV, and wind power production. The PDF is extra separated into subdivisions to contract the dissimilar situations of loading, PV, and wind speed [35]:

### *3.1 Load demand modeling*

The doubt about the model of load demand via the PDF is clear as follows [35]:

$$f_d(P_d) = \frac{1}{\sigma_d \sqrt{2\pi}} exp\left[-\frac{(P_d-\mu_d)^2}{2\sigma_d{}^2}\right] \quad (12)$$

where $\mu_d$ and $\sigma_d$ specified the mean and the standard deviation parameters with values ($\mu_d = 70$ and $\sigma_d = 10$). while, $P_d$ denotes the probability density of the typical distribution load, one-to-one. Load demand probability and probable load situation could be reached by employing the next:

$$\tau_{d,i} = \int_{P_{d,i}{}^{min}}^{P_{d,i}{}^{max}} f_d(P_d).dP_d \quad (13)$$

$$P_{d,i} = \frac{1}{\tau_{d,i}} \int_{P_{d,i}{}^{min}}^{P_{d,i}{}^{max}} P_d * f_d(P_d).dP_d \quad (14)$$

where $P_{d,i}{}^{max}$ and $P_{d,i}{}^{min}$ represent the border limits of interval i.

### *3.2 Wind speed modeling*

To model a wind farm, first, the wind speed must be modeled. The wind speed has a random behavior. Proper modeling should be done to obtain the output wind plant. The Weibull Probability Distribution Function (PDF) is careful here to model the doubt of the wind speed (m/sec); the expression is clear as follows [35],[47-49]:

$$f_v(v) = (\frac{\beta}{\alpha})(\frac{v}{\alpha})^{\beta-1} exp\left[-(\frac{v}{\alpha})^{\beta}\right] \ , 0 \le v < \infty \quad (15)$$

wherever, α, β are the Weibull PDF mounting and shaping parameters. As a function of wind speed, the output of wind turbine power can be single-minded as follows:

$$P_w(v_w) = \begin{cases} 0 & , for\ v_w < v_{wi}\ and\ v_w > v_{wo} \\ P_{wr}\left(\frac{v_w - v_{wi}}{v_{wr} - v_{wi}}\right) & , for\ v_{wi} \le v_w \le v_{wr} \\ P_{wr} & , for\ v_{wr} \le v_w \le v_{wo} \end{cases} \quad (16)$$

where, $P_{wr}$ is the wind turbine-rated output power with a value of ($P_{wr} = 3W$), $v_{wi}$, $v_{wo}$ and $v_{wr}$ are the wind turbine cut-in, cut-out, and rated speeds, with values of ( 3m/s, 25m/s, and 16m/s) respectively. The probability of wind speed is calculated using the following equations:

$$\tau_{wind,k} = \int_{v_k{}^{min}}^{v_k{}^{min}} f_v(v).dv \quad (17)$$

where, $v_k{}^{min}$ , $v_k{}^{min}$ denote the initial and final points of wind speed's interlude at $k^{th}$ scenario, $\tau_{w,k}$ is the probability of the wind speed being in scenario k.

### *3.3 Solar Irradiance modeling*

Design of the solar irradiation doubt can be reached employing the lognormal PDF as follows [35]:

$$f_G(P_d) = \frac{1}{G\sigma_s\sqrt{2\pi}} exp\left[-\frac{(lnG - \mu_s)^2}{2\sigma_s{}^2}\right] \text{ for } G > 0 \quad (18)$$

where $\mu_s$ and $\sigma_s$ indicated the mean and standard deviation parameters of the random variables, with values ($\mu_s = 5.5$ and $\sigma_s = 0.5$). respectively.

The PV arrangement production power as a function of irradiation can be designed via the next equations:

$$P_s(G) = \begin{cases} P_{sr}\left(\frac{G^2}{G_{std} \times X_c}\right) for\ \ 0 < G \le X_c \\ P_{sr}\left(\frac{G}{G_{std}}\right) \qquad for\ \ G \ge X_c \end{cases} \quad (19)$$

where, $G_{std}$ is the standard solar irradiation 1000 W/m$^2$ while $X_c$ means a certain irradiation point set as 120 W/m$^2$. $P_{sr}$, is the PV arrangement output power. Calculating the solar irradiation probability might be achieved:

$$\tau_{Solar,m} = \int_{G_m{}^{min}}^{G_m{}^{max}} f_G(G).dG \tag{20}$$

where $G_m{}^{max}$ and $G_m{}^{min}$ are solar irradiance limits of a state $m$.

*3.4 Combined load generation modeling*

The matching probabilities designed for load demand, wind speed models, and solar irradiance can be attained by combining the model of three functions and multiplying their probabilities in (13),(17), and(20), the related expression is given as follow:

$$\tau_S = \tau_{d,i} \times \tau_{wind,k} \times \tau_{Solar,m} \tag{21}$$

3.5 *correlation between DGs uncertainties*

In power systems like other systems, the system RVs may be dependent on input uncertainties. If there is a dependency, this dependence may have a positive or negative effect from one variable to another. In general, the issue of correlation in RVs is expressed and determined by the covariance matrix or correlation coefficient matrix. Correlation coefficients are presented according to (22) [42]:

$$\rho_{x,y} = \left(\frac{cov(x,y)}{\sigma_x\sigma_y}\right) = \left(\frac{E[(x-\mu_x)(y-\mu_y)]}{\sigma_x\sigma_y}\right) \tag{22}$$

The correlation coefficient ($\rho$) can be –1, +1, or between them, or zero. If it is +1, it concerns the perfect linear relation and if it is –1, it concerns the complete linear relation, and in other relations, the values between the interval [-1, 1] indicate the correlation degree.

## 4. Taguchi's Orthogonal Array Testing Method

The TM is a statistical method advanced by Dr. Genichi Taguchi to decrease the difference in industry progression over a strong strategy of research to improve product quality [43-44],[50]. The Robust Optimization (RO) or parameter optimization difficulties with an agreed computable objective function are founded on the determination of differences bound for inexact parameters, consequently, the doubts are controlled by a predetermined parameter which is called the uncertainty budget that shows the boundaries. With the TM method, dissimilar stages are careful with individual doubt parameters or random variables (RVs). Concerning these stages, dissimilar situations or experimentations of the problem are careful. For (RO) the TM of experimental design employs orthogonal arrangements (OAs) to tune the input parameters over dissimilar stages and quickly optimize these fluctuating factors to become the optimal outcome or the objective function in a minimum number of experiments [51-53]. The basic TM is broadly divided into two essential steps, i.e., Orthogonal Array (OA) construction, and response analysis.

*4.1 Orthogonal Arrays*

An (OA) denoted by the letter L is a fractional factorial matrix whose rows represent factor levels in each run and its columns represent a specific factor whose levels change in each experiment. All traditional factorial designs and fraction arrays are orthogonal [42]. Based on OAs, TOAT is an effective method for converting the uncertainties to deterministic values; in this method, with a minimum number of experiments OAs determine the minimum number of uncertain values. In general, the (OA) with dimension $L_e y^u$ refers to u uncertain parameters, each parameter has y levels for an e experiments arrangement. $L_4 2^3$ is the smallest OA, which refers to executing 4 experiments with three 2-level parameters, such as shown in Table 1. The word factor in the TOAT refers to a random variable (RV), while the amount given by the probability distribution is indicated by the word level [54].

**Table 1.** The Taguchi Orthogonal array $L_4 2^3$

| Number of experiments | Level of each factor (variable) | | |
|---|---|---|---|
| | Factor 1 ( RV1) | Factor 2 ( RV2) | Factor 3 ( RV3) |
| 1 | 1 | 1 | 1 |
| 2 | 1 | 2 | 2 |
| 3 | 2 | 1 | 2 |
| 4 | 2 | 2 | 1 |

In general, the relationship between input and output RVs in a distribution network according to (23):

$$Y_{in} = f(X_{out}) \tag{23}$$

The input and output factors (RVs) vectors are $Y_{in}$ and $X_{out}$, respectively, and $f$ is a nonlinear relation that establishes the relationship between $X_{out}$ and $Y_{in}$.

The POPF of a distribution system including PV and WT DGs is investigated and analyzed by TM based on OA, each experiment refers to a load flow, and on the other hand, because the distribution networks are three-phase, for each phase, if we have many factors (RVs) for a three-phase distribution network, their number will increase, so the number of tests and the number of load flow will increase and as a result, the final answer will be obtained after a long time and many calculations. OAs can be used to dramatically reduce the number of experiments to get the answer instead of all the tests so that these OAs get the same answer by performing a very small number of tests in less time and calculations than all experiments can be achieved [42].

*4.2 TM Response Analysis With Popf*

Three steps can be taken using TOAT to get certain parameters from uncertain ones, these steps are:

*4.2.1 First Step: Determining the levels number of each factor (RV)*

Determination of the levels number for each factor is the primary stage using the TOAT for solving a probabilistic power flow. Using TOAT, minimal calculations can be achieved using 2-level parameters, while using 3-level parameters leads to long time computation [42],[54].

*4.1.2 Second step: Factors levels (RVs) Determination*

Determination of the levels of the factors is the second step using the TOAT. Two levels of a random variable (RV) can be made using a probabilistic Gaussian distribution function. In this case, the normal distribution or Gaussian probabilistic distribution function can model the load demand because it is a symmetric continuous distribution, and the two levels of the demand load (2-level experiments) are assumed as μ + σ and μ − σ, in that order. The wind speed is modeled using the Weibull continuous distribution function. The μ and σ describe the mean and standard deviation values of the Gaussian probabilistic distribution function [54].

*4.1.3 Step three: Design of optimal experiment*

An approximate solution to the probabilistic power flow with the best performance index is obtained in this step. In TM, the final optimal answer was reached using an optimal experiment based on the optimal levels of RVs instead of all experiments based on OAs. Three steps lead to an optimal experiment, as follows [42], [54]:

1) For each experiment, a performance index is defined in this step as follows:

$$Y_j = \sum_{L=1}^{NL} \left| f_{jL} - f_L^* \right| , j=1,2,3,....,N \quad (24)$$

wherever N denotes the number of the experiment, NL represents the branches number, $\boldsymbol{f_L}^*$ represents the nominal power movement at line L. $\boldsymbol{f_{jL}}$ indicates the power flow at line L attained from the calculations of the power flow concerning experiment j.

2) In the next step, calculations of the average effects of the factors stages on performance indicators are made. For the sample, in Table 1 the average effects of the levels of the factors, for four experiments, are definite as the set of Equations (25), in which the average effects of dissimilar levels of factors on the performance indicators are defined as:

$$\left\{ \begin{array}{l} \bar{A}_1 = \frac{(Y_1+Y_2)}{2}, \quad \bar{A}_2 = \frac{(Y_3+Y_4)}{2} \\ \bar{B}_1 = \frac{(Y_2+Y_4)}{2}, \ \bar{B}_2 = \frac{(Y_1+Y_3)}{2} \\ \bar{C}_1 = \frac{(Y_2+Y_3)}{2}, \quad \bar{C}_2 = \frac{(Y_1+Y_4)}{2} \end{array} \right\} \quad (25)$$

3) The focal effect of a separate factor on the performance indicators $\boldsymbol{Y_j}$ is obtained in this step, by subtracting the second-level effect from the first-level effect using the set of Equations (26) as follows:

$$\left\{ \begin{array}{l} \Delta A = (\bar{A}_2 - \bar{A}_1), \\ \Delta B = (\bar{B}_2 - \bar{B}_1), \\ \Delta C = (\bar{C}_2 - \bar{C}_1), \end{array} \right. \quad (26)$$

In the optimal experiment, the first level of a factor or RV is considered if the main effect of this factor is negative, and the second level of this factor is considered if the main effect is positive. Finally, figure (1) explains the Flowchart of the Taguchi method.

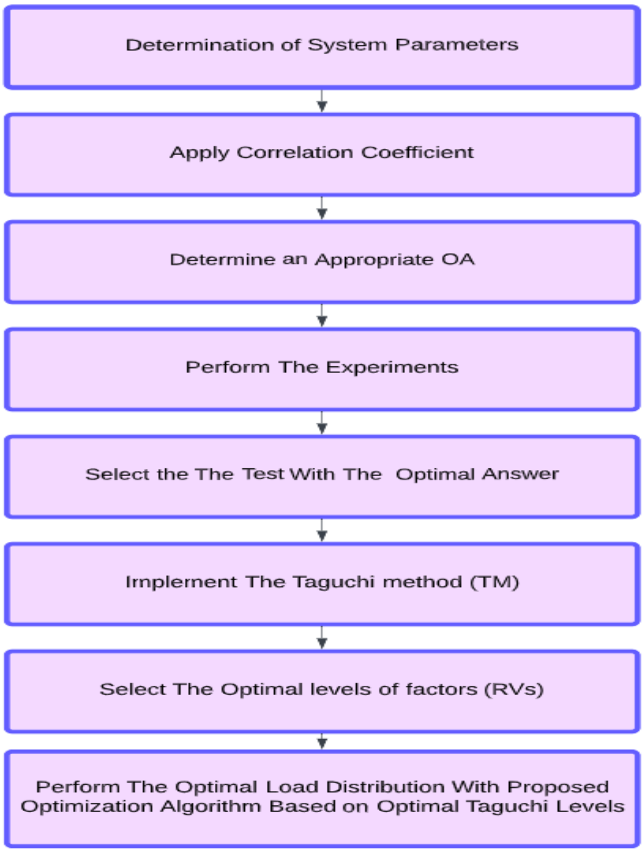


**Fig. 1.** Flowchart of the Taguchi method.

## 5. Dandelion Optimizer (DO) Overview

A new swarm intelligence bioinspired optimization algorithm that has low computational time and high convergence speed are called the Dandelion Optimizer (DO). The dandelion algorithm updated the next generation of individuals by dynamically regulating the seeding radius of dandelions and their autonomous learning. And based on it, a variant dandelion algorithm divided the population of dandelions into two subgroups: core dandelion and assistant dandelion, and these two types of dandelion are applied in different ways to sow seeds. The two dandelion populations complement each other and coevolve to fully extend the search range, which increases the probability of finding the optimal location. Two types of seeds are generated to avoid falling into local optimal and keep the diversity of seeds, and the selection strategy is a mechanism for keeping diversity. Therefore, the DA has the capability of avoiding premature convergence. The proposed DO algorithm is introduced recently and it has three stages presented as follows and explained in table (2) [55]:

1. Rising stage: In this stage, seeds raise spirally because of the eddies from above. Seeds also, in his stage, may drift locally in communities based on weather conditions.
2. Descending stage: Flying seeds, in this stage, descend steadily and adjust their direction constantly in the global space.
3. landing stage: In this stage, seeds land randomly so that they grow. A Levy random walk and Brownian motion describe the movement of a seed in the landing and descending stages. CEC2017 benchmark

functions are used for the performance evaluation of Dandelion Optimizer, including the stability, optimization accuracy, scalability, and convergence, through a comparison with nine known nature-inspired metaheuristic algorithms.

$$X_{t+1} = X_t + \alpha * v(x) * v(y) * lnY(X_s - X_t) \quad (27)$$

$$a = rand() * \left(\frac{1}{T^2}t^2 - \frac{2}{T}t + 1\right) \quad (28)$$

$$X_{t+1} = X_t * k \quad (29)$$

$$X_{t+1} = X_t - \alpha * \beta_t * (X_{mean,t} - \alpha * \beta_t * X_t) \quad (30)$$

$$X_{t+1} = X_{elite} + \alpha * leuy(\lambda) * (X_{elite} - X_t * \delta) \quad (31)$$

**Table 2.** Dandelion Optimizer (DO)

| |
|---|
| **Algorithm** Dandelion Optimizer |
| **Input**: the population size pop, the maximum number of iterations T, and variable dimension Dim |
| **Output**: the optimal dandelion seed $X_{best}$ and itsfitness value $f_{best}$ |
| 1: Initialize dandelion seed X of DO. |
| 2: Calculate the fitness value f of each dandelion seed. |
| 3: Select the optimum dandelion seed $X_{elite}$ according to fitness values |
| 4: **while** (t < T) **do** |
| /***Rise stage***/ |
| 5: **if** randn() <1.5 **do** |
| 6: Generate adaptive parameters using Eq.(28) |
| 7: Update dandelion seeds using Eq.(27) |
| 8: **else if do** |
| 9: Generate adaptive parameters using Eq.(28) |
| 10: Update dandelion seeds using Eq.(29) |
| 11: **end if** |
| /***Decline stage***/ |
| 12: Update dandelion seeds using Eq.(30) |
| /***Land stage***/ |
| 13: Update dandelion seeds using Eq.(31) |
| 14:Arrange dandelion seeds from good to bad according to fitness |
| 15: Update $X_{elite}$ |
| 16: **if** f($X_{elite}$) < f($X_{best\ t}$) |
| 17: $X_{best} = X_{elite}$ , $f_{best} = f_{elite}$ |
| 18: **end if** |
| 19: **end while** |
| 20: **Return** $X_{best}$ and $f_{best}$ |

## 6. Results and Discussions

To achieve the (TM) efficiency, the 30- bus IEEE standard system has been used. which consists of 6 generators with one slack bus, 37 branches of transmission lines 4 branches of tap changing transformers, and 9 reactive power compensators. The system has a total power demand of 238.4 MW and 126.2 MVAR. Buses and lines, for the proposed IEEE 30-bus system shown in figure (2), have detailed data which are defined in [56],[57]. The initial reactive power loss of the network without the presence of WTs is 22.244 MVAR and the initial active power loss is 17.59 MW. This system consists of 19 control variables including 9 shunt VAR capacitors, 4 settings of tap changing transformers and 6 generators with limitations values introduces in a table (3). Aditionaly, load data of the IEEE30- bus system, wind speed and solar irradiation data for 24 hours periods are indicated in table (5) and table (5) respectively.

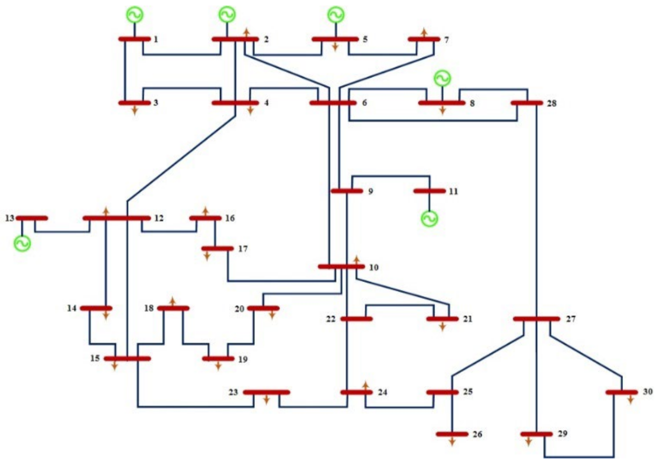


**Fig. 2.** Standard IEEE-30 bus test system

The TM is implemented in MATLAB and MINITAB software. In this case, there are two wind farms on buses 29, and 30 and a PV cell on bus 16, which has a nominal capacity of 10 MW. To simulate this wind farm and PV cell, data are received from the North Dekta site and the Watford area [58]. The average wind speed in this area is 8.5 m/s and the standard deviation is 5.55. The frequency of one-year wind speeds is seen in figure (3), and the right skewness of this information is quite clear. The optimal reactive power dispatch obtained from the TM test with DO will be equal to 17.5 MW, which is the number of system losses from the test instead of 27.5 in Ref [42]. And the levels determined by the TM are obtained, but the answer that we obtain for the losses of the same system from the normal OPRD by the Newton-Raphson load flow method is equal to 33 MW, and this indicates that TM adjusts the POPF of factor levels in such a way that the least number of losses occur in the system and reduces the difference between 33 and 17.5, which is equal to 15.5 MW, which is a large number of losses.

**Table 3.** Limitations of control variables

| Control Variables | Min. value | Max. value |
|---|---|---|
| $V_{G1}$ (pu) | 0.95 | 1.1 |
| $V_{G2}$ (pu) | 0.95 | 1.1 |
| $V_{G5}$ (pu) | 0.95 | 1.1 |
| $V_{G8}$ (pu) | 0.95 | 1.1 |
| $V_{G11}$ (pu) | 0.95 | 1.1 |
| $V_{G13}$ (pu) | 0.95 | 1.1 |
| $T_{11}$ (6-9) | 0.9 | 1.1 |

| | | |
|---|---|---|
| $T_{12}$ (6-10) | 0.9 | 1.1 |
| $T_{15}$ (4-12) | 0.9 | 1.1 |
| $T_{36}$ (28-27) | 0.9 | 1.1 |
| $Q_{C10}$ (MVAR) | 0 | 5 |
| $Q_{C12}$ (MVAR) | 0 | 5 |
| $Q_{C15}$ (MVAR) | 0 | 5 |
| $Q_{C17}$ (MVAR) | 0 | 5 |
| $Q_{C20}$ (MVAR) | 0 | 5 |
| $Q_{C21}$ (MVAR) | 0 | 5 |
| $Q_{C23}$ (MVAR) | 0 | 5 |
| $Q_{C24}$ (MVAR) | 0 | 5 |
| $Q_{C29}$ (MVAR) | 0 | 5 |

**Table 4.** Bus load data of the IEEE 30-bus system

| Bus NO | Load | | Bus NO | Load | |
|---|---|---|---|---|---|
| | P (MW) | Q (MVAr) | | P (MW) | Q (MVAr) |
| **1** | **0.0** | **0.0** | **16** | **3.5** | **1.8** |
| **2** | **21.7** | **12.7** | **17** | **9.0** | **5.8** |
| **3** | **2.4** | **1.2** | **18** | **3.2** | **0.9** |
| **4** | **67.6** | **1.6** | **19** | **9.5** | **3.4** |
| **5** | **94.2** | **19.0** | **20** | **2.2** | **0.7** |
| **6** | **0.0** | **0.0** | **21** | **17.5** | **11.2** |
| **7** | **22.8** | **10.9** | **22** | **0.0** | **0.0** |
| **8** | **30.0** | **30.0** | **23** | **3.2** | **1.6** |
| **9** | **0.0** | **0.00** | **24** | **8.7** | **6.7** |
| **10** | **5.8** | **2.0** | **25** | **0.0** | **0.0** |
| **11** | **0.0** | **0.0** | **26** | **3.5** | **2.3** |
| **12** | **11.2** | **7.5** | **27** | **0.0** | **0.0** |
| **13** | **0.0** | **0.0** | **28** | **0.0** | **0.0** |
| **14** | **6.2** | **1.6** | **29** | **2.4** | **0.9** |
| **15** | **8.2** | **2.5** | **30** | **10.6** | **1.9** |

**Table 5.** Wind Speed and Solar Irradiation Data for 24-Hour Period

| Hour | Wind speed (m/s) | Solar radiation ($w/m^2$) | Hour | Wind speed (m/s) | Solar radiation ($w/m^2$) |
|---|---|---|---|---|---|
| 1 | 5.7 | 0 | 13 | 5.9 | 833 |
| 2 | 6.5 | 0 | 14 | 4.9 | 850 |
| 3 | 7.5 | 0 | 15 | 3.5 | 680 |
| 4 | 6.9 | 0 | 16 | 3.4 | 595 |
| 5 | 8.6 | 93.5 | 17 | 2.8 | 255 |
| 6 | 10.5 | 212.5 | 18 | 3.1 | 212.5 |
| 7 | 13.6 | 255 | 19 | 2.3 | 153 |
| 8 | 10.4 | 467.5 | 20 | 2.9 | 68 |
| 9 | 9.1 | 637.5 | 21 | 3.5 | 42.5 |
| 10 | 9.3 | 680 | 22 | 3.8 | 0 |
| 11 | 7.7 | 816 | 23 | 3.8 | 0 |
| 12 | 7.0 | 850 | 24 | 4.8 | 0 |

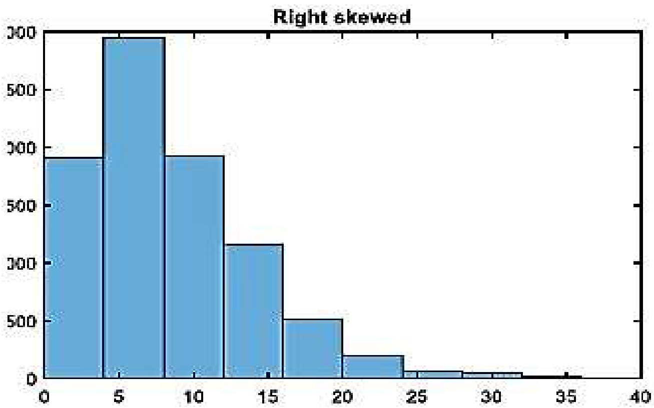


**Fig. 3.** Wind speed frequency diagram.

*6.1 Case 1: Real Power Losses Saving*

Real power loss lessen was the deemed target here. The DO algorithm was used to accomplish the best solution, Table 6 gives the results. The DO algorithm is useful for establishing the perfect settings of the control variable, which diminishes the losses of the system. As a result, when the DO algorithm is used, real power losses are dramatically lowered from a value of 27.5 MW to 17.5 MW. In figure 4, real power losses utilizing the DO method are steeply converged while taking other comparative techniques into account. The optimum solution can be achieved using the algorithm within 100 iterations, which demonstrates the rapid convergence of the DO algorithm. The evaluated real power loss is compared to that found using before-published population-based optimization techniques to evaluate the performance of the approach. Table 6 shows how the DO algorithm outperforms these prior methods. Particularly, the majority of acquired solutions using heuristic optimization algorithms are feasible, primarily due to voltage magnitude accepted at all system load buses as shown in figure 5.

**Table 6.** Optimal control variables for minimizing active power losses for IEEE 30-bus test system

| Control Variables | DO | GA | KWA |
|---|---|---|---|
| $V_{G1}$ (pu) | 1.099999 | 1.100000 | 1.10000 |
| $V_{G2}$ (pu) | 1.08096 | 1.081147 | 1.08083 |
| $V_{G5}$ (pu) | 1.050073 | 1.049857 | 1.04987 |
| $V_{G8}$ (pu) | 1.0581226 | 1.057884 | 1.05801 |
| $V_{G11}$ (pu) | 1.09999 | 1.10000 | 1.10000 |
| $V_{G13}$ (pu) | 1.099999 | 1.10000 | 1.10000 |
| $T_{11}$ (6-9) | 1.045711 | 0.996084 | 1.038072 |
| $T_{12}$ (6-10) | 0.90000 | 0.966384 | 0.901334 |
| $T_{15}$ (4-12) | 0.994927 | 1.007813 | 1.013492 |
| $T_{36}$ (28-27) | 0.965835 | 0.971414 | 0.967464 |
| $Q_{C10}$ (MVAR) | 4.999999 | 3.320597 | 2.52272 |
| $Q_{C12}$ (MVAR) | 4.999999 | 5 | 4.21918 |
| $Q_{C15}$ (MVAR) | 5 | 4.8406 | 3.59157 |
| $Q_{C17}$ (MVAR) | 4.99999 | 4.95720 | 1.39472 |
| $Q_{C20}$ (MVAR) | 4.779537 | 4.10309 | 4.65710 |
| $Q_{C21}$ (MVAR) | 4.999999 | 4.9999 | 3.73254 |
| $Q_{C23}$ (MVAR) | 3.57303 | 3.74637 | 1.38789 |
| $Q_{C24}$ (MVAR) | 4.999999 | 4.9939 | 2.23654 |
| $Q_{C29}$ (MVAR) | 2.010295 | 2.08777 | 0.98210 |
| **Power Loss (MW)** | **17.541** | **17.5459** | **17.5977** |
| Voltage Deviation (pu) | 2.1908 | 2.08468 | 1.93747 |
| **Control Variables** | **DO** | **PDO** | **WOA** |
| $V_{G1}$ (pu) | 1.099999 | 1.10000 | 1.0999 |
| $V_{G2}$ (pu) | 1.08096 | 1.10000 | 1.08093 |
| $V_{G5}$ (pu) | 1.050073 | 1.10000 | 1.04992 |
| $V_{G8}$ (pu) | 1.0581226 | 1.10000 | 1.05827 |
| $V_{G11}$ (pu) | 1.09999 | 1.07152 | 1.10000 |
| $V_{G13}$ (pu) | 1.099999 | 1.1000 | 1.09999 |
| $T_{11}$ (6-9) | 1.045711 | 1.02608 | 1.0033 |
| $T_{12}$ (6-10) | 0.90000 | 1.10000 | 0.948889 |
| $T_{15}$ (4-12) | 0.994927 | 1.10000 | 1.001595 |
| $T_{36}$ (28-27) | 0.965835 | 1.10000 | 0.969088 |
| $Q_{C10}$ (MVAR) | 4.999999 | 4.70967 | 4.72722 |
| $Q_{C12}$ (MVAR) | 4.999999 | 0 | 4.93047 |
| $Q_{C15}$ (MVAR) | 5 | 2.9317 | 4.65465 |
| $Q_{C17}$ (MVAR) | 4.99999 | 4.9949 | 4.988412 |
| $Q_{C20}$ (MVAR) | 4.779537 | 4.9989 | 4.875829 |
| $Q_{C21}$ (MVAR) | 4.999999 | 4.9998 | 4.995757 |
| $Q_{C23}$ (MVAR) | 3.57303 | 4.52031 | 3.830656 |
| $Q_{C24}$ (MVAR) | 4.999999 | 4.78674 | 4.981892 |
| $Q_{C29}$ (MVAR) | 2.010295 | 4.31481 | 2.292923 |
| **Power Loss (MW)** | **17.541** | **18.32097** | **17.543448** |
| Voltage Deviation (pu) | 2.1908 | 1.60716 | 2.161373 |

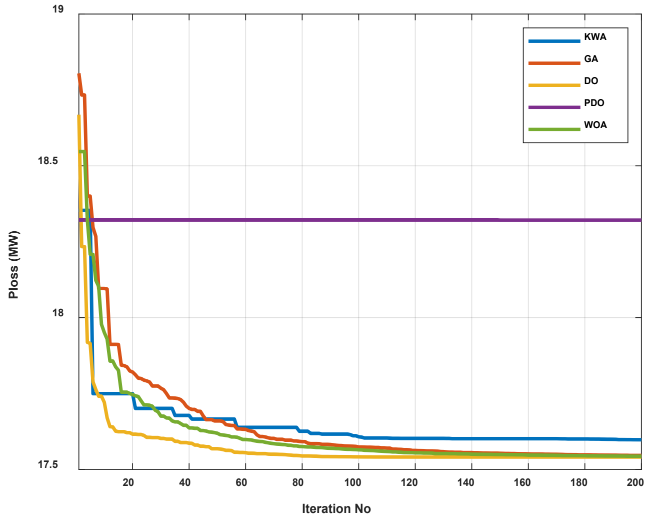


**Fig. 4.** The DO and compared algorithms convergence characteristics for case 1.

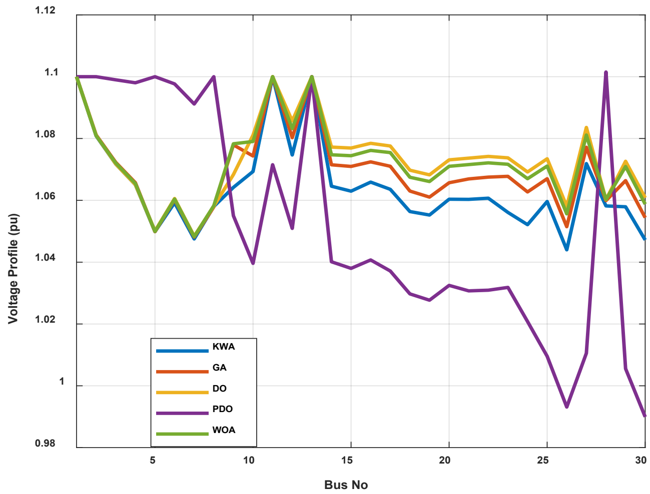


**Fig. 5.** The standard IEEE-30 bus voltage profile for case 1.

### *6.2 Case 2: Reactive Power Losses Saving*

Reactive power loss lessen was the deemed target here. The DO algorithm was used to accomplish the best solution, Table 7 gives the results. The DO algorithm is useful for establishing the perfect settings of the control variable, which diminishes losses of the system. As a result, when the DO algorithm is used, reactive power losses are dramatically lowered to 13.5 MVAR. In figure 6, reactive power losses utilizing the DO method are steeply converged while taking other comparative techniques into account. The optimum solution can be achieved using the algorithm within 60 iterations, which demonstrates the rapid convergence of the DO algorithm. The evaluated reactive power loss is compared to that found using published population-based optimization techniques to evaluate the performance of the approach. Table 7 shows how the DO algorithm outperforms these prior methods. Particularly, the majority of acquired solutions using heuristic optimization algorithms are feasible, primarily due to voltage magnitude accepted at all system load buses as shown in figure 7.

**Table 7.** Optimal control variables for minimizing reactive power losses for IEEE 30-bus test system.

| **Control Variables** | **DO** | **GA** | **KWA** |
|---|---|---|---|
| $V_{G1}$ (pu) | 1.09999 | 1.09999 | 1.10000 |
| $V_{G2}$ (pu) | 1.09991 | 1.09931 | 1.09998 |
| $V_{G5}$ (pu) | 1.08038 | 1.07817 | 1.08042 |
| $V_{G8}$ (pu) | 1.09277 | 1.09185 | 1.09260 |
| $V_{G11}$ (pu) | 1.10000 | 1.09940 | 1.10000 |
| $V_{G13}$ (pu) | 1.09999 | 1.09983 | 1.10000 |
| $T_{11}$ (6-9) | 0.99035 | 0.98955 | 0.98932 |
| $T_{12}$ (6-10) | 0.98809 | 0.98534 | 0.98767 |
| $T_{15}$ (4-12) | 0.98710 | 0.98818 | 0.98657 |
| $T_{36}$ (28-27) | 0.98193 | 0.97676 | 0.97883 |
| $Q_{C10}$ (MVAR) | 4.99999 | 4.85294 | 4.9999 |
| $Q_{C12}$ (MVAR) | 4.99999 | 3.92603 | 0.91544 |
| $Q_{C15}$ (MVAR) | 4.99999 | 3.31971 | 4.47127 |
| $Q_{C17}$ (MVAR) | 4.99999 | 3.58234 | 2.07193 |
| $Q_{C20}$ (MVAR) | 5 | 3.25223 | 4.93287 |
| $Q_{C21}$ (MVAR) | 4.99999 | 4.55178 | 0.93451 |
| $Q_{C23}$ (MVAR) | 4.99999 | 4.93390 | 3.52795 |
| $Q_{C24}$ (MVAR) | 4.99999 | 4.52366 | 0.21669 |
| $Q_{C29}$ (MVAR) | 4.99999 | 2.91758 | 1.11625 |
| **Reactive Loss (MVAR)** | **13.5127** | **13.7754** | **14.4338** |
| Power Loss (MW) | 17.9542 | 17.9363 | 18.0441 |
| Voltage Deviation (pu) | 1.09999 | 2.55203 | 2.37778 |
| **Control Variables** | **DO** | **PDO** | **WOA** |
| $V_{G1}$ (pu) | 1.09999 | 1.100000 | 1.099999 |
| $V_{G2}$ (pu) | 1.09991 | 1.100000 | 1.099948 |
| $V_{G5}$ (pu) | 1.08038 | 1.100000 | 1.080532 |
| $V_{G8}$ (pu) | 1.09277 | 1.100000 | 1.092786 |
| $V_{G11}$ (pu) | 1.10000 | 1.100000 | 1.099929 |
| $V_{G13}$ (pu) | 1.09999 | 1.100000 | 1.100000 |
| $T_{11}$ (6-9) | 0.99035 | 1.100000 | 0.990286 |
| $T_{12}$ (6-10) | 0.98809 | 1.100000 | 0.989363 |
| $T_{15}$ (4-12) | 0.98710 | 1.100000 | 0.987491 |
| $T_{36}$ (28-27) | 0.98193 | 1.100000 | 0.981429 |
| $Q_{C10}$ (MVAR) | 4.99999 | 4.845026 | 4.990179 |
| $Q_{C12}$ (MVAR) | 4.99999 | 4.774687 | 5 |
| $Q_{C15}$ (MVAR) | 4.99999 | 4.953949 | 4.984691 |
| $Q_{C17}$ (MVAR) | 4.99999 | 4.99808 | 4.987528 |
| $Q_{C20}$ (MVAR) | 5 | 4.81635 | 4.997664 |
| $Q_{C21}$ (MVAR) | 4.99999 | 4.89972 | 5 |
| $Q_{C23}$ (MVAR) | 4.99999 | 4.85877 | 4.996899 |
| $Q_{C24}$ (MVAR) | 4.99999 | 4.99411 | 4.999124 |
| $Q_{C29}$ (MVAR) | 4.99999 | 4.74025 | 5 |
| **Reactive Loss (MVAR)** | **13.5127** | **20.0528** | **13.51449** |
| Power Loss (MW) | 17.9542 | 18.3867 | 17.95597 |
| Voltage Deviation (pu) | 1.09999 | 1.63176 | 2.677833 |

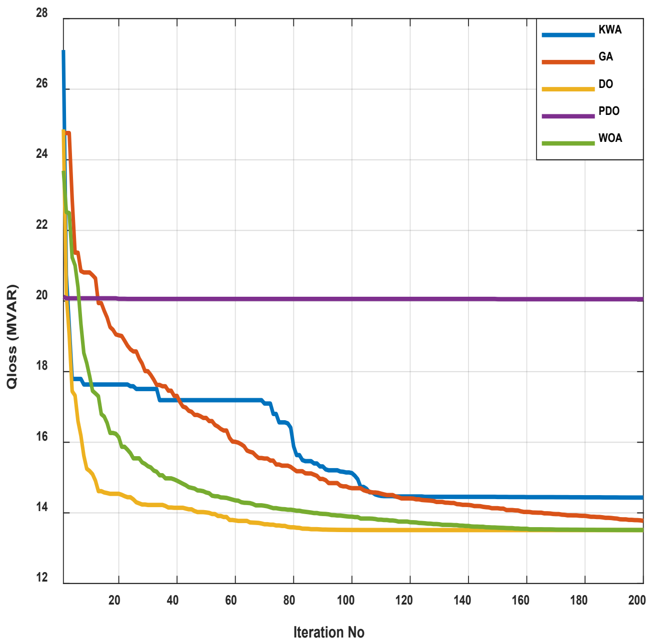


**Fig. 6.** The DO and compared algorithms convergence characteristics for case 2.

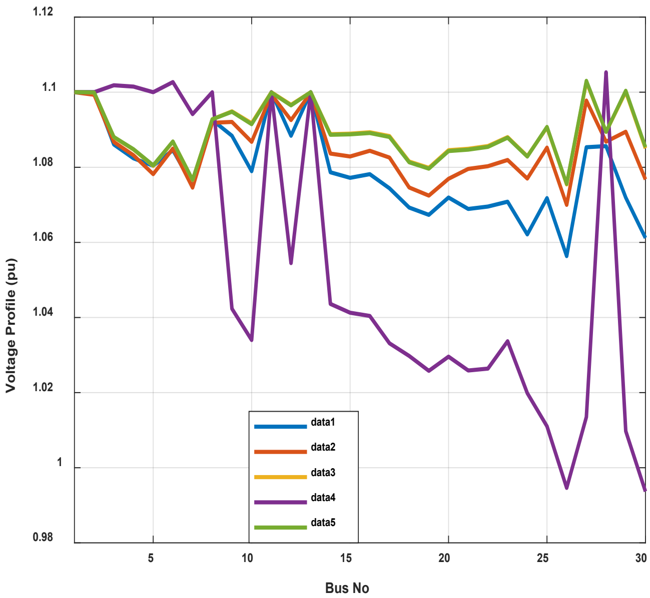


**Fig. 7.** The standard IEEE-30 bus voltage profile for case 2.

*6.3 Case 3: Voltage Deviation Minimization*

The aim function to be improved using the DO algorithm in this part is increasing voltage deviation. Figure 8 illustrates the pattern of increasing system voltage divergence. The findings mentioned in Table 8 point out that the voltage deviation index is decreased to 0.13 pu by using the DO algorithm. The DO method significantly outperforms other population-based optimization strategies in Table 8's comparison of solutions obtained using these two methods. Particularly, the all of acquired solutions using heuristic optimization algorithms are feasible, primarily due to the voltage magnitude accepted at all system load buses as shown in figure 9.

Table 8. Optimal control variables for minimizing voltage

deviation for IEEE 30-bus test system

| Control Variables | DO | GA | KWA |
|---|---|---|---|
| $V_{G1}$ (pu) | 1.00000 | 1.00014 | 1.000017 |
| $V_{G2}$ (pu) | 1.0000 | 1.0003 | 1.00052 |
| $V_{G5}$ (pu) | 0.9999 | 1.000117 | 1.000104 |
| $V_{G8}$ (pu) | 1.02098 | 1.014429 | 1.025153 |
| $V_{G11}$ (pu) | 1.00000 | 1.00082 | 1.000014 |
| $V_{G13}$ (pu) | 1.00000 | 1.01877 | 1.000664 |
| $T_{11}$ (6-9) | 1.01228 | 0.98861 | 0.9724426 |
| $T_{12}$ (6-10) | 0.90142 | 0.91200 | 0.9000709 |
| $T_{15}$ (4-12) | 0.96617 | 0.99929 | 0.9513557 |
| $T_{36}$ (28-27) | 0.9614 | 0.97444 | 0.9696701 |
| $Q_{C10}$ (MVAR) | 5 | 1.45107 | 0.7455046 |
| $Q_{C12}$ (MVAR) | 4.99999 | 4.86673 | 4.9252119 |
| $Q_{C15}$ (MVAR) | 4.99998 | 4.99045 | 4.59508 |
| $Q_{C17}$ (MVAR) | 0.79706 | 3.35794 | 1.571298 |
| $Q_{C20}$ (MVAR) | 4.9998 | 5 | 4.999126 |
| $Q_{C21}$ (MVAR) | 4.9997 | 4.160617 | 3.587489 |
| $Q_{C23}$ (MVAR) | 4.9999 | 4.997928 | 1.664685 |
| $Q_{C24}$ (MVAR) | 5 | 4.999554 | 1.327213 |
| $Q_{C29}$ (MVAR) | 0.2452 | 2.203964 | 2.650459 |
| Power Loss (MW) | 23.0167 | 22.71428 | 23.3087 |
| **Voltage Deviation (pu)** | **0.13082** | **0.149252** | **0.174027** |
| **Control Variables** | **DO** | **PDO** | **WOA** |
| $V_{G1}$ (pu) | 1.00000 | 1.00000 | 1.000662 |
| $V_{G2}$ (pu) | 1.0000 | 1.00000 | 1.0003178 |
| $V_{G5}$ (pu) | 0.9999 | 1.00000 | 1.0002348 |
| $V_{G8}$ (pu) | 1.02098 | 1.04955 | 1.0198592 |
| $V_{G11}$ (pu) | 1.00000 | 0.99999 | 1.0000317 |
| $V_{G13}$ (pu) | 1.00000 | 0.99606 | 1.0002497 |
| $T_{11}$ (6-9) | 1.01228 | 1.02228 | 1.00442548 |
| $T_{12}$ (6-10) | 0.90142 | 0.90000 | 0.92452426 |
| $T_{15}$ (4-12) | 0.96617 | 0.943387 | 0.96106441 |
| $T_{36}$ (28-27) | 0.9614 | 0.987448 | 0.96465907 |
| $Q_{C10}$ (MVAR) | 5 | 4.00088 | 4.9781617 |
| $Q_{C12}$ (MVAR) | 4.99999 | 3.07594 | 3.7961058 |
| $Q_{C15}$ (MVAR) | 4.99998 | 4.99251 | 4.9528035 |
| $Q_{C17}$ (MVAR) | 0.79706 | 2.89759 | 3.54518 |
| $Q_{C20}$ (MVAR) | 4.9998 | 1.60741 | 5 |
| $Q_{C21}$ (MVAR) | 4.9997 | 2.89741 | 4.97129 |
| $Q_{C23}$ (MVAR) | 4.9999 | 2.75707 | 5 |
| $Q_{C24}$ (MVAR) | 5 | 2.200368 | 5 |
| $Q_{C29}$ (MVAR) | 0.2452 | 2.56376 | 0.7127106 |
| Power Loss (MW) | 23.0167 | 24.2969 | 22.91436 |
| **Voltage Deviation (pu)** | **0.13082** | **0.211148** | **0.13621378** |

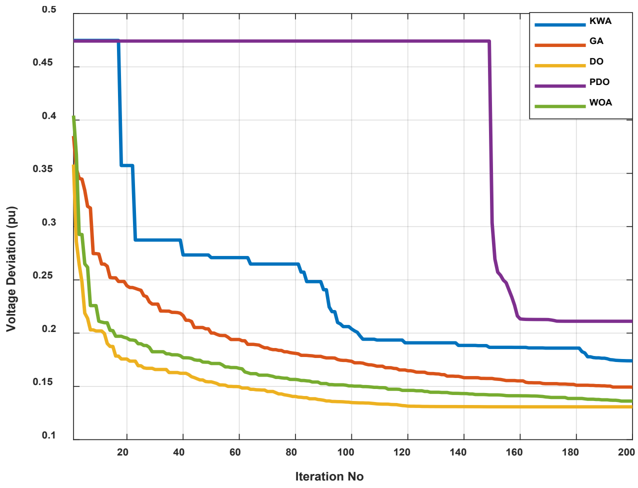


**Fig. 8** The DO and compared algorithms convergence characteristics for case 3.

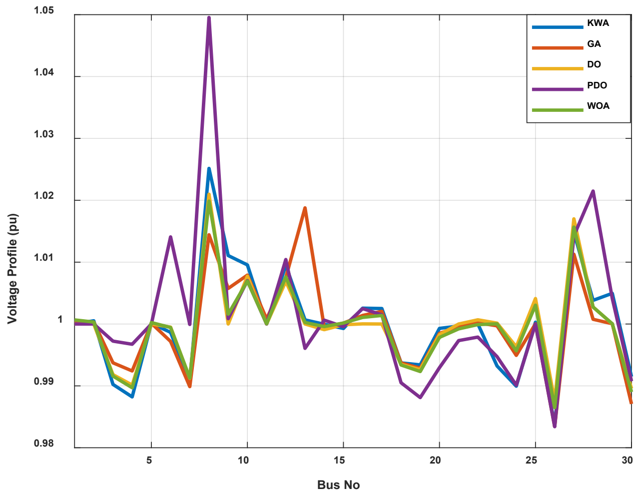


**Fig. 9** The standard IEEE-30 bus voltage profile for case 3.

## 7. Conclusion

In this research, an efficient and novel optimization optimizer known as DO is developed for handling ORPD optimization issues. Furthermore, four algorithms GA, KWA, PDO, and WOA are compared with the DO algorithm for addressing a single objective ORPD issue have been proposed and evaluated on a modified IEEE 30-bus test system in the presence of RESs using the taguchi method which is based on orthogonal arrays considering the uncertainty of RES and load profile. The supremacy and efficacy of DO have been evaluated for optimizing three single-objective functions to prove its efficiency and lead to achieving minimization of active power, reactive power, and voltage deviation. According to the comparison results, the DO gives, in all cases, better performance in minimizing the objective functions than other algorithms. It can be concluded that the DO solved the OPRD in a short period of time, indicating that the DO can be succeded in other real-life applications such as PV parameter estimation, PI parameter tuning, management applications such as energy management and load management, conventional and smart grid applications, industry, and engineering applications.

**References**

[1] J. Sun, M. Mihret, M. Cespedes, D. Wong, and M. Kauffman, "Data Center Power System Stability—Part II: System Modeling and Analysis," CSEE Journal of Power and Energy Systems, vol. 8, no. 2, pp. 420-438, 2022.

[2] F. O. Igbinovia, G. Fandi, J. Švec, Z. Müller, and J. Tlusty, "Comparative review of reactive power compensation technologies," in 2015 16th International Scientific Conference on Electric Power Engineering (EPE), 2015: IEEE, pp. 2-7.

[3] Z. Qu et al., "Dynamic exploitation Gaussian bare-bones bat algorithm for optimal reactive power dispatch to improve the safety and stability of power system," IET Renewable Power Generation, vol. 16, no. 7, pp. 1401-1424, 2022.

[4] K. Lee and Y. Han, "Reactive-power-based robust MTPA control for v/f scalar-controlled induction motor drives," IEEE Transactions on Industrial Electronics, vol. 69, no. 1, pp. 169- 178, 2021.

[5] S. Saodah, I. M. W. Kastawan, E. Yusuf, B. P. Manunggal, and M. Maryanti, "Simulation of Effects of Using Capacitor for Reactive Power (VAR) Compensation on Electrical Power Supply Quality," in 5th FIRST T1 T2 2021 International Conference (FIRST-T1-T2 2021), 2022: Atlantis Press, pp. 168-174.

[6] M. Fernando, D. Gamini, and J. Naveendra, "Reduction of Reactive Power Waste of Inductive Electrical Appliances using Power Factor Correction," Vidyodaya Journal of Science, vol. 24, no. 01, 2021.

[7] R. Verma and N. P. Padhy, "Optimal Power Flow Based DR in Active Distribution Network With Reactive Power Control," IEEE Systems Journal, 2021.

[8] Y. Liu, D. Ćetenović, H. Li, E. Gryazina, and V. Terzija, "An optimized multi-objective reactive power dispatch strategy based on improved genetic algorithm for wind power integrated systems," International Journal of Electrical Power & Energy Systems, vol. 136, p. 107764, 2022.

[9] A. A. Ogunsina, M. O. Petinrin, O. O. Petinrin, E. N. Offornedo, J. O. Petinrin, and G. O. Asaolu, "Optimal distributed generation location and sizing for loss minimization and voltage profile optimization using ant colony algorithm," SN Applied Sciences, vol. 3, no. 2, pp. 1-10, 2021.

[10] R. Wagle, P. Sharma, C. Sharma, T. Gjengedal, and C. Pradhan, "Bio-inspired hybrid BFOA- PSO algorithm-based reactive power controller in a standalone wind-diesel power system," International Transactions on Electrical Energy Systems, vol. 31, no. 3, p. e12778, 2021.

[11] G. Chen, J. Cao, and Z. Zhang, "Application of global best imperialist competition algorithm for multi-objective reactive power optimization," in 2018 Chinese Automation Congress (CAC), 2018: IEEE, pp. 1240-1245.

[12] Y. Li, B. Sun, Y. Zeng, S. Dong, S. Ma, and X. Zhang, "Active distribution network active and reactive power coordinated dispatching method based on discrete monkey algorithm," International Journal of Electrical Power & Energy Systems, vol. 143, p. 108425, 2022.

[13] M. H. Jahangir, S. Eslamnezhad, S. A. Mousavi, and M. Askari, "Multi-year sensitivity evaluation to supply prime and deferrable loads for hospital application using hybrid renewable energy systems," Journal of Building Engineering, vol. 40, p. 102733, 2021.

[14] Y. Zhang, L. Wang, H. Ding, Y. Zhu, Q. Hu, and Z. Lv, "An Overview of Virtual Power Plant Prospects from the Perspective of Optimal Scheduling, Market Bidding and Transient Analysis," in 2021 IEEE Sustainable Power and Energy Conference (iSPEC), 2021: IEEE, pp. 281-286.

[15] R. Vempalle and P. Dhal, "Optimal analysis of time varying load radial distribution system with photovoltaic and wind generating system using novel hybrid optimization technique," Renewable Energy Focus, vol. 41, pp. 246-257, 2022.

[16] Y. Shi, H. D. Tuan, A. V. Savkin, C.-T. Lin, J.

[17] G. Zhu, and H. V. Poor, "Distributed model predictive control for joint coordination of demand response and optimal power flow with renewables in smart grid," Applied Energy, vol. 290, p. 116701, 2021.

[18] A. Ranjbar, S. Vig, and K. Sharma, "Performance Analysis of Grid Connected Distributed Generation Sources (DGS) Using ETAP," in Cognitive Informatics and Soft Computing: Springer, 2022, pp. 105-114.

[19] A. Angulo, D. Rodríguez, W. Garzón, D. F. Gómez, A. Al Sumaiti, and S. Rivera, "Algorithms for bidding strategies in local energy markets: Exhaustive search through parallel computing and metaheuristic optimization," Algorithms, vol. 14, no. 9, p. 269, 2021.

[20] R. M. Barros, G. G. Lage, and R. d. A. L. Rabêlo, "Sequencing paths of optimal control adjustments determined by the optimal reactive dispatch via Lagrange multiplier sensitivity analysis," European Journal of Operational Research, vol. 301, no. 1, pp. 373-385, 2022.

[21] A. Islam, O. Das, and N. Mohammad, "Optimized Energy Generation and Power Flow Model to Minimize Power System Operation Cost," in 2021 5th International Conference on Electrical Information and Communication Technology (EICT), 2021: IEEE, pp. 1-6.

[22] S. Pan, Z. Li, J. Zheng, R. Wu, X. Zhou, and Y. Zhang, "A Non-iterative Solution Method for DC Optimal Power Flow Based on Holomorphic Embedding," in 2021 IEEE 5th Conference on Energy Internet and Energy System Integration (EI2), 2021: IEEE, pp. 1865- 1870.

[23] W. Lu, K. Xie, M. Liu, X. Wang, and L. Cheng, "Online decentralized tracking for nonlinear time-varying optimal power flow of coupled transmission-distribution grids," arXiv preprint arXiv:2208.02008, 2022.

[24] L. Bobo, A. Venzke, and S. Chatzivasileiadis, "Second-order cone relaxations of the optimal power flow for active distribution grids: Comparison of methods," International Journal of Electrical Power & Energy Systems, vol. 127, p. 106625, 2021.

[25] T. Xu et al., "Optimal capacity allocation of energy storage in distribution networks considering active/reactive coordination," Energies, vol. 14, no. 6, p. 1611, 2021.

[26] S. J. Chia, S. Abd Halim, H. M. Rosli, and N. A.

[27] M. Kamari, "Power Loss Minimization using Optimal Power Flow based on Firefly Algorithm," International Journal of Advanced Computer Science and Applications, vol. 12, no. 9, 2021.

[28] R. Taghavi, H. Samet, A. R. Seifi, and Z. M. Ali, "Stochastic Optimal Power Flow in Hybrid Power System Using Reduced-Discrete Point Estimation Method and Latin Hypercube Sampling," IEEE Canadian Journal of Electrical and Computer Engineering, vol. 45, no. 1, pp. 63-67, 2021.

[29] J. Jithendranath, D. Das, and J. M. Guerrero, "Probabilistic optimal power flow in islanded microgrids with load, wind and solar uncertainties including intermittent generation spatial correlation," Energy, vol. 222, p. 119847, 2021.

[30] X. Mo, T. Liu, and X. Lyu, "ATC-Based Scenario Decomposition Algorithm for Optimal Power Flow of Distribution Networks Considering High Photovoltaic Penetration," arXiv preprint arXiv:2207.03686, 2022.

[31] B. Xia, Y. Chen, W. Yang, Q. Chen, X. Wang, and K. Min, "Stochastic Optimal Power Flow for Power Systems Considering Wind Farms Based on the Stochastic Collocation Method," IEEE Access, vol. 10, pp. 44023-44032, 2022.

[32] K. Lenin, "Hybridization of Genetic Particle Swarm Optimization Algorithm with Symbiotic Organisms Search Algorithm for Solving Optimal Reactive Power Dispatch Problem," Journal of Applied Science, Engineering, Technology, and Education, vol. 3, no. 1, pp. 12-21, 2021.

[33] T. T. Nguyen and D. N. Vo, "Improved social spider optimization algorithm for optimal reactive power dispatch problem with different objectives," Neural Computing and Applications, vol. 32, no. 10, pp. 5919-5950,2020.

[34] Y. Zhou, J. Zhang, X. Yang, and Y. Ling, "Optimal reactive power dispatch using water wave optimization algorithm," Operational Research, vol. 20, no. 4, pp. 2537-2553, 2020.

[35] Z. Li, Y. Cao, L. V. Dai, X. Yang, and T. T. Nguyen, "Finding solutions for optimal reactive power dispatch problem by a novel improved antlion optimization algorithm," Energies, vol. 12, no. 15, p. 2968, 2019.

[36] L. Lian, "Reactive power optimization based on adaptive multi-objective optimization artificial immune algorithm," Ain Shams Engineering Journal, vol. 13, no. 5, p. 101677, 2022.

[37] M. H. Hassan, S. Kamel, M. A. El-Dabah, T. Khurshaid, and J. L. Domínguez-García, "Optimal reactive power dispatch with time- varying demand and renewable energy uncertainty using Rao-3 algorithm," IEEE Access, vol. 9, pp. 23264-23283, 2021.

[38] L. Kanagasabai, "Heat transfer and simulated coronary circulation system optimization algorithms for real power loss reduction," 2021.

[39] H. Yapici, "Solution of optimal reactive power dispatch problem using pathfinder algorithm," Engineering Optimization, vol. 53, no. 11, pp. 1946-1963, 2021.

[40] A. M. Abd-El Wahab, S. Kamel, M. H. Hassan, M. I. Mosaad, and T. A. AbdulFattah, "Optimal Reactive Power Dispatch Using a Chaotic Turbulent Flow of Water-Based Optimization Algorithm," Mathematics, vol. 10, no. 3, p. 346, 2022.

[41] M. Marzband, A. Sumper, A. Ruiz-Álvarez, J. L. Domínguez-García, and B. Tomoiagă, "Experimental evaluation of a real time energy management system for stand-alone microgrids in day-ahead markets," Applied Energy, Vol. 106, pp. 365-376, 2013.

[42] Y. Che, X. Wang, X. Lv, and Y. Hu, "Probabilistic load flow using improved three point estimate method," International Journal of Electrical Power & Energy Systems, Vol. 117, p. 105618, 2020.

[43] G. Carpinelli, R. Rizzo, P. Caramia, and P. Varilone, "Taguchi's method for probabilistic three-phase power flow of unbalanced distribution systems with correlated Wind and Photovoltaic Generation Systems," Renewable Energy, Vol. 117, pp. 227–241, 2018.

[44] M. Najjarpour, B. Tousi, and S. Jamali, "Loss Reduction in Distribution Networks With DG Units by Correlating Taguchi Method and Genetic Algorithm," Iranian Journal of Electrical and Electronic Engineering, Vol. 18, No. 4, p. 2429, 2022.

[45] NAND K. MEENA , ANIL SWARNKAR, JIN YANG, NIKHIL GUPTA , and K. R. NIAZI , "Modified Taguchi-Based Approach for Optimal Distributed Generation Mix in Distribution Networks," IEEE Access, Vol. 7, pp. 135689–135702, 2019.

[46] Juan Carlos Beltrána , Andrés Julián Aristizábala , Alejandra Lópezb , Mónica Castanedaa , Sebastián Zapataa , Yulia Ivanovac, "Comparative analysis of deterministic and probabilistic methods for the integration of distributed generation in power systems," Energy Reports, Vol. 6, pp. 104–104, 2020.

[47] Hoa M. Nguyen, Tien N. Nguyen , and Hoan V. Pham, "Decentralized Optimal Dispatch of Reactive Power Sources in Power Systems Based on Augmented Lagrangian Method," INTERNATIONAL JOURNAL of RENEWABLE ENERGY RESEARCH, Vol.12, No.2, June 2022.

[48] Ahmed Gad, Hossam A.Gabbar, "Approximate Power Loss Minimization in Radial Distribution Networks Using the Feeder Reconfiguration," 2020 IEEE 8th International Conference on Smart Energy Grid Engineering (SEGE), Oshawa, ON, Canada, 12-14 August 2020.

[49] Umesh Mohankumar, Athul M. V., Joshua Freeman, Balakrishnan Shankar, Krishnashree Achuthan, "Remote Triggered Monitoring of Wind Performance Using Weibull and Rayleigh Distributions," 2017 IEEE 6th International Conference on Renewable Energy Research and Applications (ICRERA), San Diego, CA, USA, 05-08 November 2017.

[50] Elmer Rodrigo Aquino Larico, "Wind Energy Potential by the Weibull Distribution at High-Altitude Peruvian Highlands," INTERNATIONAL JOURNAL of SMART GRID, Vol.5, No.3, September, 2021 .

[51] F. Tooryan, E. Randolph Collins, A. Ahmadi and Shriram S. Rangarajan, " Distributed Generators Optimal Sizing and Placement in A Microgrid Using PSO," 2017 IEEE 6th International Conference on Renewable Energy Research and Applications (ICRERA), San Diego, CA, USA, 05-08 November 2017.

[52] Sumod Pawar , Dr. Jitendra Hole , Mangesh Bankar,"A Taguchi Method Optimization for Engine Parameters of VCR Engine Fuelled with Xanthium strumarium L. Oil Biodiesel Blend," INTERNATIONAL JOURNAL of RENEWABLE ENERGY RESEARCH, Vol.12, No.3, September, 2022.

[53] Derong Liu, and Ying Cai, " Taguchi Method for Solving the Economic Dispatch Problem With Nonsmooth Cost Functions," IEEE TRANSACTIONS ON POWER SYSTEMS, VOL. 20, NO. 4, NOVEMBER 2005.

[54] Hamid Reza Nikzad, Hamdi Abdi, and Shahriar Abbasi, " Robust Unit Commitment Applying Information Gap Decision Theory and Taguchi Orthogonal Array Technique," Robust Optimal Planning and Operation of Electrical Energy Systems, Springer, 2019.

[55] Nand K. Meena, Anil Swarnkar, Nikhil Gupta, Khaleequr R. Niazi, " Multi-objective Taguchi approach for optimal DG integration in distribution systems," IET Generation, Transmission & Distribution, Vol. 11, Iss. 9, pp. 2418–2428, 2017.

[56] SARA-SADAT GHASEMI, AND HAMDI ABDI, " Robust security constrained optimal power flow considering load and wind power generation uncertainties by applying Taguchi method," Journal of Energy Management and Technology (JEMT), Vol. 5, Issue 1, pp. 51–61, 2020.

[57] S. Zhao, T. Zhang, S. Ma, and M. Chen, "Dandelion Optimizer: A nature-inspired metaheuristic algorithm for engineering applications," Engineering Applications of Artificial Intelligence, vol. 114, p. 105075, 2022.

[58] Abd-El Wahab, A. M., Kamel, S., Hassan, M. H., Mosaad, M. I., & Abdulfattah, T. A "Optimal Reactive Power Dispatch Using a Chaotic Turbulent Flow of Water-Based Optimization Algorithm," Mathematics, VOL. 10, NO. 3,(2022).

[59] Khan, N. H., Wang, Y., Tian, D., Raja, M. A. Z., Jamal, R., & Muhammad, Y. "Design of Fractional Particle Swarm Optimization Gravitational Search Algorithm for Optimal Reactive Power Dispatch Problems," IEEE Access, VOL. 8, pp.146785–146806, (2020).

[60] J. Solc and B. W. Botnen, "JV Task 99- Integrated Risk Analysis and Contaminant Reduction, Watford City, North Dakota," Univ. of North Dakota, Grand Forks, ND (United States), 2007.